Virology 441 (2013) 152–161

Contents lists available at SciVerse ScienceDirect

Virology

journal homepage: www.elsevier.com/locate/yviro

Ophioviruses CPsV and MiLBVV movement protein is encoded in RNA 2 and interacts with the coat protein

Gabriel Robles Luna [a,1], Eduardo José Peña [b,1], María Belén Borniego [a], Manfred Heinlein [b], Maria Laura Garcia [a,*]

[a] Instituto de Biotecnología y Biología Molecular, CCT—La Plata CONICET, Fac. Cs. Exactas, U.N.L.P., Calles 49 y 115, La Plata, Argentina
[b] Institut de Biologie Moléculaire des Plantes du CNRS (UPR 2357), Université de Strasbourg, 12 rue du Général Zimmer, 67084 Strasbourg Cedex, France

ARTICLE INFO

Article history:
Received 2 February 2013
Returned to author for revisions
8 March 2013
Accepted 21 March 2013
Available online 18 April 2013

Keywords:
Ophioviridae
Negative-strand RNA virus
Citrus psorosis virus
Mirafiori lettuce big-vein virus
Movement protein
Protein–protein Interaction

ABSTRACT

Citrus psorosis virus (CPsV) and *Mirafiori lettuce big-vein virus* (MiLBVV), members of the *Ophioviridae* family, have segmented negative-sense single-stranded RNA genomes. To date no reports have described how ophioviruses spread within host plants and/or the proteins involved in this process. Here we show that the 54K protein of CPsV is encoded by RNA 2 and describe its subcellular distribution. Upon transient expression in *Nicotiana benthamiana* epidermal cells the 54K protein, and also its 54K counterpart protein of MiLBVV, localize to plasmodesmata and enhance GFP cell-to-cell diffusion between cells. Both proteins, but not the coat proteins (CP) of the respective viruses, functionally *trans*-complement cell-to-cell movement-defective *Potato virus X* (PVX) and *Tobacco mosaic virus* (TMV) mutants. The 54K and 54K proteins interact with the virus-specific CP in the cytoplasm, suggesting a potential role of CP in ophiovirus movement. This is the first study characterizing the movement proteins (MP) of ophioviruses.

Introduction

Ophioviruses are the causal agents of important diseases affecting lettuce, citrus and ornamental plants. *Citrus psorosis virus* (CPsV), the type member of the *Ophioviridae* family, causes one of the most widespread and economically important viral diseases of citrus (Alioto et al., 2007; Zanek et al., 2006). *Mirafiori lettuce big-vein virus* (MiLBVV) and *Lettuce ring necrosis virus* (LRNV), two other members of this family, are the causal agent of big-vein disease (Roggero et al., 2000) and lettuce necrosis (Torok and Vetten, 2010; Torok and Vetten, 2002; Torok and Vetten, 2003), respectively, and *Freesia sneak virus* is associated with a severe disease called freesia leaf necrosis (Vaira et al., 2009; Vaira et al., 2007). FreSV, LRNV and MiLBVV are transmitted by the root-infecting fungal parasite *Olpidium brassicae* (Bos and Huijberts, 1996; Lot et al., 2002; van Dorst, 1975); whereas the vectors of CPsV and *Ranunculus white mottle virus* (RWMV) are still unknown.

The ophiovirus genome is divided into three or four ssRNA segments of negative polarity (Kormelink et al., 2011). CPsV has three genomic RNAs; RNA 1 encodes a 24 kDa polypeptide of unknown function and, separated by an intergenic region, the putative RNA-dependent RNA polymerase (RdRp) of 280 kDa (Naum-Ongania et al., 2003). RNA 2 encodes a polypeptide of 53.7 kDa (54K^{CPsV} protein) of unknown function (Sánchez de la Torre et al., 2002), and the RNA 3 of CPsV encodes the coat protein of 48.6 kDa (CP^{CPsV}) (Sánchez de la Torre et al., 1998). MiLBVV and LRNV have a similar genome organization which, in addition, consists of a fourth RNA segment (RNA 4) (van der Wilk et al., 2002). According to bioinformatic analysis, the RNA 2 genome segments of MiLBVV and LRNV encode 54K protein (54K^{MiLBVV}) and 50 K (50 K^{LRNV}) proteins, respectively, in the complementary strand, and the functions of these proteins have not been determined. Like for CPsV, the RNA 3 of these two ophioviruses also encodes coat protein, i.e. a CP of 48.5 kDa in the case of MiLBVV (CP^{MiLBVV}) and a CP of 48 kDa in the case of LRNV.

For successful infection, plant viruses must be able to replicate and to move their genomes between cells and tissues. Cell-to-cell movement of viruses occurs through plasmodesmata (PD), dynamic channels in the cell wall providing membrane and cytoplasmic continuity between neighboring cells. Although the overall size exclusion limit (SEL) of PD is determined by the developmental and physiological status of the leaf, the conductivity of the channels is highly flexible and can be altered by non-cell autonomous proteins (NCAPs) (Lucas et al., 2009) that include the movement proteins (MP) of plant viruses. The MP of *Tobacco mosaic virus* (TMV) was the first identified MP (MP^{TMV}) (Deom

* Corresponding author.
E-mail addresses: garcia_m@biol.unlp.edu.ar, marialauragarcia2010@gmail.com (M.L. Garcia).
[1] Equal contributors.

0042-6822/$ - see front matter © 2013 Elsevier Inc. All rights reserved.
http://dx.doi.org/10.1016/j.virol.2013.03.019

et al., 1987; Meshi et al., 1987). Today we know that plant viruses encode one or more MPs capable of exploiting cellular mechanisms for macromolecular targeting and transport through PD and to distant tissues (Lucas, 2006; Niehl and Heinlein, 2011). It has been shown that MPs accumulate at PD and increase their SEL essential for virus movement (Derrick et al., 1992; Poirson et al., 1993; Vaquero et al., 1994; Wolf et al., 1989).

To date, no reports have described how CPsV or other ophioviruses spread within host plants and also the viral proteins required for ophiovirus movement are yet unknown. Here, we demonstrate that the predicted RNA 2-encoded protein (54K) is indeed expressed in CPsV infected tissue. Moreover, using confocal laser scanning microscopy (CLSM) of the $54K^{CPsV}$ or $54K^{MiLBVV}$ proteins tagged with fluorescent proteins we show that these proteins are localized to PD, suggesting that they are involved in ophiovirus movement. We show that upon transient expression in *Nicotiana benthamiana* both proteins spread to neighbouring epidermal cells and promote the cell-to-cell trafficking of GFP *in trans*. The two proteins are also capable to *trans*-complement the intercellular movement of MP-deficient *Potato virus X* (PVX) and TMV mutants. Using fluorescent lifetime imaging microscopy (FLIM) and co-immunoprecipitation analysis we demonstrate that the $54K^{CPsV}$ and $54K^{MiLBVV}$ proteins can interact with CP^{CPsV} and CP^{MiLBVV}, respectively. Collectively, these observations indicate that the $54K^{CPsV}$ and $54K^{MiLBVV}$ proteins function as MP of the respective viruses and suggest a potential role of the viral CP in virus movement.

Results

Identification of $54K^{CPsV}$ protein during infection and upon ectopic expression

Using a previously generated polyclonal serum against the $54K^{CPsV}$ protein (Peña et al., 2012b) in Western blot assays, an immunoreactive band of the expected size was detected in crude extracts of infected, but not in mock-inoculated, *Chenopodium quinoa* leaves, confirming the expression during infection of the predicted protein. The protein is detected after 4 days post inoculation (dpi) (Fig. 1) coincident with the time of appearance of first symptoms (chlorotic local lesions) and detection of CP^{CPsV} (Peña et al., 2012b).

Localization of 54K and 54K proteins tagged with fluorescent markers

To increase subcellular resolution, we studied the localization of transiently expressed $54K^{CPsV}$ and $54K^{MiLBVV}$ proteins fused to fluorescent proteins in *N. benthamiana* epidermal cells by CLSM. The DNA constructs encoding the fusion proteins are shown in Fig. 2. eGFP:$54K^{CPsV}$ co-localizes with co-expressed free mRFP in the cytoplasm and nucleus (Fig. 3A). A similar localization to the cytoplasm and nucleus was also found for the eGFP:$54K^{MiLBVV}$

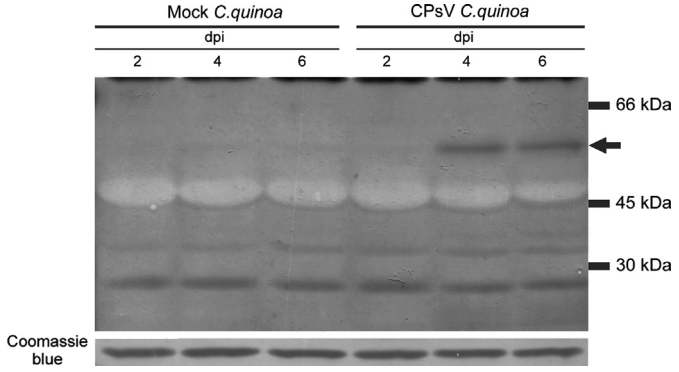

Fig. 1. Detection of $54K^{CPsV}$ protein in infected *C. quinoa*. Western blot analysis of crude extracts of CPsV-infected and mock-inoculated *C. quinoa* plants at 2, 4 and 6 dpi. Molecular weight markers are shown on the right of the figure. Arrows indicate the location of $54K^{CPsV}$. Coomassie blue staining was used as loading control.

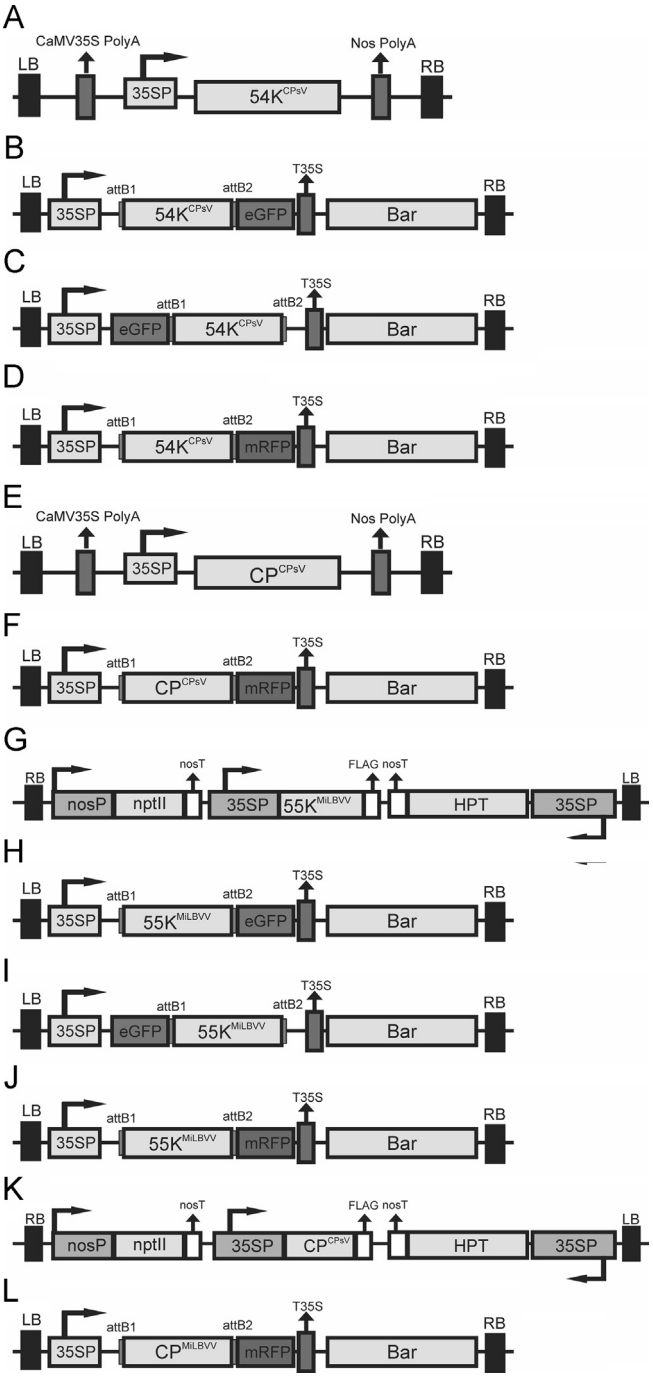

Fig. 2. DNA constructs. Schematic representation of the T-DNA region in the binary plasmids for transient expression of $54K^{CPsV}$ (A) and CP^{CPsV} (E) proteins; C-terminal GFP fusion proteins: $54K^{CPsV}$:eGFP (B), $54K^{MiLBVV}$:eGFP (H); C-terminal mRFP fusion proteins: $54K^{CPsV}$:mRFP (D), CP^{CPsV}:mRFP (F), $54K^{MiLBVV}$:mRFP (J), CP^{MiLBVV}:mRFP (L); N-terminal GFP fusion proteins: eGFP:$54K^{CPsV}$ (C), eGFP:$54K^{MiLBVV}$ (I); and C-terminal FLAG fusion proteins: $54K^{MiLBVV}$:FLAG (G), CP^{MiLBVV}:FLAG (K). Abbreviations: nosP, *nopaline synthase* promoter; nosT, *nopaline synthase* terminator; 35SP, 35S *Cauliflower mosaic virus* (CaMV) promoter; T35S, 35S CaMV terminator; CaMV35S PolyA, CaMV polyA signal; Nos PolyA, *nopaline synthase* polyA signal; FLAG, FLAG epitope; LB, left border; RB, right border; Bar, *phosphinothricin acetyl transferase* gene; HPT, *hygromycin phosphotransferase* gene; attb1, recombination site 1; attb2, recombination site 2; eGFP, enhanced green fluorescent protein; mRFP, monomeric red fluorescent protein.

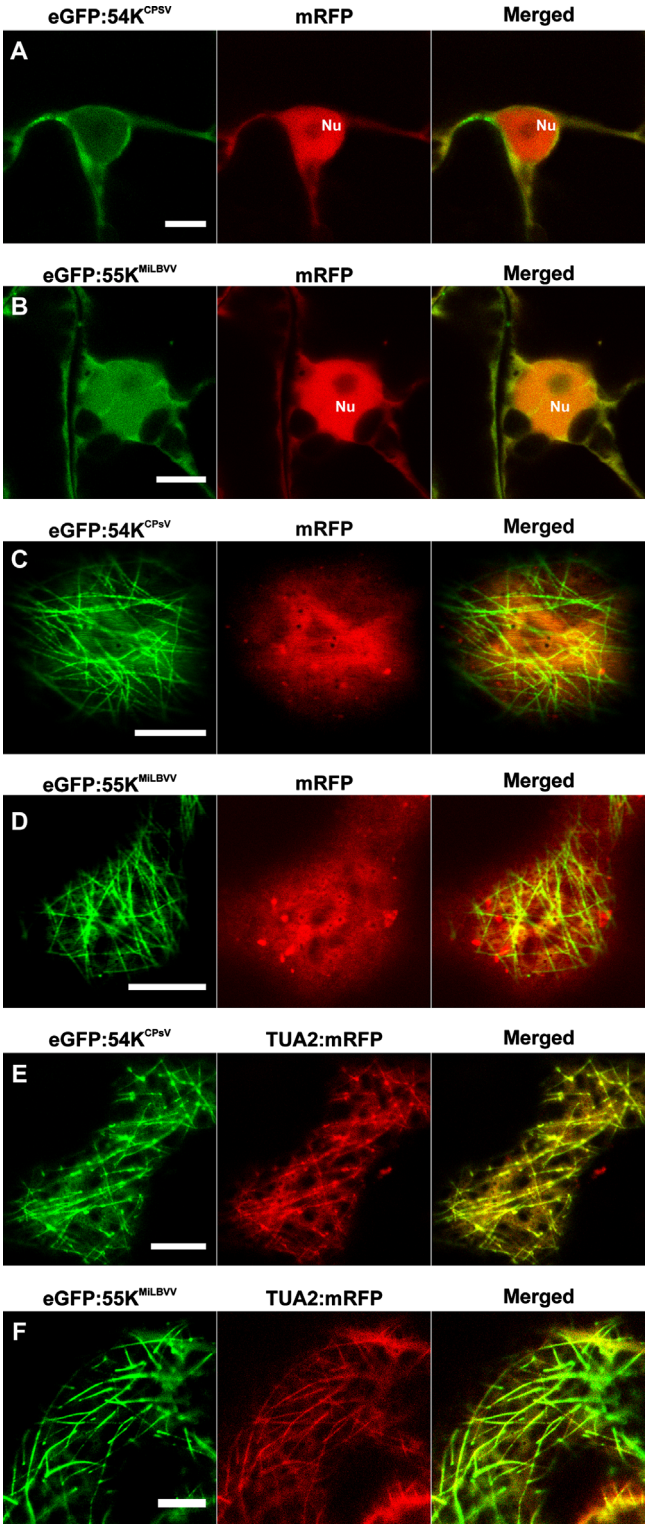

Fig. 3. Subcellular localization of fluorescent protein-tagged 54K^{CPsV} and 54K^{MiLBVV}. Co-expression of eGFP:54K^{CPsV} (A) or eGFP:54K^{MiLBVV} (B) with free mRFP (nucleo cytoplasmic marker) at 2 dpai in *N. benthamiana* epidermal cell, showing co-localization at these locations. Cortical view of these cells showing filaments for eGFP:54K^{CPsV}(C) and eGFP:54K^{MiLBVV} (D). Co-expression of eGFP:54K^{CPsV} (E) or eGFP:54K^{MiLBVV} (F) with TUA2:mRFP at 3 dpai in *N. benthamiana* epidermal cells. Scale bar = 10 μm. Nu = nucleus; TUA2:mRFP, alpha-tubulin fused to mRFP.

protein (Fig. 3B). Interestingly, in the cortical cytoplasm the eGFP:54K^{CPsV} and eGFP:54K^{MiLBVV} proteins even co-expressed with mRFP were found in association with filaments (Fig. 3C and D). To know the identity of these filaments, co-expression with the microtubule marker TUA2:mRFP (Van Damme et al., 2004) was assayed, finding co-localization (Fig. 3E and F) which indicates that these proteins interact indirectly or directly with microtubules. The observation was the same irrespective whether the proteins were fused at their N- or C-terminus with eGFP or to the C-terminus to mRFP (data not shown).

Further analysis using plasmodesmata callose binding protein 1 (PDCB1) as PD marker (Simpson et al., 2009) revealed that 54K^{CPsV} and 54K^{MiLBVV} co-localize with PDCB1:mCherry to small dots at the cell wall of the epidermal cells (Fig. 4A and E, respectively). In order to confirm PD localization of eGFP:54K^{CPsV} and eGFP:54K^{MiLBVV}, the cells were subjected to plasmolysis, which causes the retraction of the plasma membrane from the cell wall except from PD. As shown in Fig. 4B and F, the fluorescence emitted from both eGFP and mCherry was retained at the cell wall, indicating that the 54K^{CPsV} and 54K^{MiLBVV} proteins accumulate at PD. Whereas PDCB1:mCherry is observed at the PD neck regions as previously demonstrated by electron microscopy (Simpson et al., 2009), the eGFP:54K^{CPsV}- and eGFP:54K^{MiLBVV}-emitted fluorescence is rather observed in between the fluorescence signal emitted from PDCB1:mCherry, thus suggesting that the proteins localize to the inner channel of PD (Fig. 4B and F zoomed upper right panels). Further evidence supporting this observation was obtained by co-localization with plasmodesmata-located protein 1 (PDLP1), other PD marker that has been previously shown to be located inside PD (Maule et al., 2011; Thomas et al., 2008). Co-expression analyses for 54K^{CPsV} and 54K^{MiLBVV} with PDLP1, shows a clear co-localization (Fig. 4C and G, respectively). When cells were plasmolyzed 54K^{CPsV} and 54K^{MiLBVV} were found to co-localize with PDLP1 at the PD channel, (Fig. 4D and H zoomed upper right panels) showing a clearly different fluorescence pattern as compared to PDCB1. Thus, we conclude that 54K^{CPsV} and 54K^{MiLBVV} are located inside the PD channel, which is consistent with a role in ophiovirus cell-to-cell movement.

The 54K^{CPsV} and 54K^{MiLBVV} proteins cause increased cell-to-cell diffusion of GFP and move between cells themselves

PD in tobacco sink leaves allows the passage of GFP (27 kDa) and other molecules of up to 50 kDa, whereas in source leaves GFP is restricted to the GFP-expressing cell (Oparka et al., 1999). Using agroinfiltration, Bayne et al. (2005) have characterized the ability of the PVX TGB1/p25 MP to facilitate the intercellular diffusion of cytosolic GFP. Thus, to determine whether the PD-localizing 54K^{CPsV} and 54K^{MiLBVV} proteins are MPs able to increase the PD SEL, we tested the ability of these proteins to facilitate the cell-to-cell diffusion of GFP. Using highly diluted cultures of *Agrobacterium tumefaciens* for agroinfiltration, we expressed GFP in isolated cells of *N. benthamiana* leaves. Under these conditions, the observed fluorescence remained almost exclusively within the transformed cells as shown in Fig. 5A and B(i), with only 13% of foci with 2 or more cells. GFP also remained in the transformed cells when leaves were co-agroinfiltrated with a high concentration of a different *Agrobacterium* culture carrying an expression construct for either CP^{CPsV} or CP^{MiLBVV} (Fig. 5A and B(i)). However, when leaves were co-agroinfiltrated with a high concentration of an *Agrobacterium* culture carrying an expression construct for either 54K^{CPsV} or 54K^{MiLBVV} protein, the GFP fluorescence was observed in clusters ranging from 2 to 7 cells in almost 90% of the evaluated foci (Fig. 5A and B(ii)), with a central highly fluorescent cell, indicating that both proteins have the capacity to facilitate GFP diffusion. To distinguish whether the 54K^{CPsV} and 54K^{MiLBVV} proteins facilitate the movement of the GFP or its mRNA, the

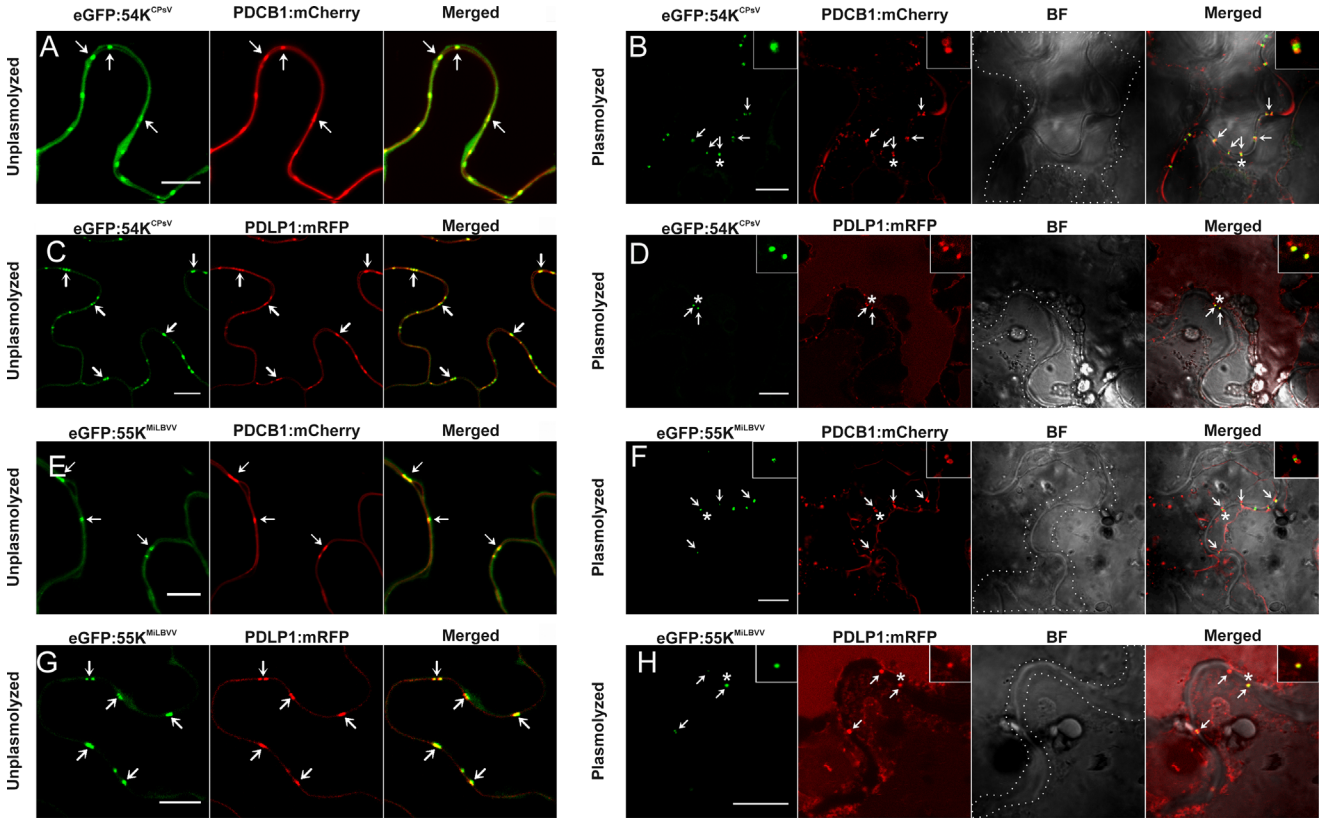

Fig. 4. 54K^{CPsV} and 54K^{MiLBVV} localize to the PD channel. Co-expression of eGFP:54K^{CPsV} with PDCB1:mCherry ((A) and (B)) or eGFP:54K^{MiLBVV} ((E) and (F)) with PDCB1:mCherry in *N. benthamiana* cells at 3 dpai. In (B) and (F) the cells were plasmolysed by infiltration of 30% glycerol solution. Scale bar = 10 μm; arrows indicate PD; the dotted lined area in bright field (BF) represents cell wall exposed after plasmolysis; asterisks indicate the zoomed PD shown at the upper right corner of (B) and (F). Co-expression of eGFP:54K^{CPsV}with PDLP1:mRFP ((C) and (D)) or eGFP:54K^{MiLBVV} ((G) and (H)) with PDLP1:mRFP in *N. benthamiana* cells at 3 dpai. In (D) and (H) the cells were plasmolysed by infiltration of 30% glycerol solution. Scale bar = 10 μm; arrows indicate PD; the dotted lined area in bright field (BF) represents cell wall exposed after plasmolysis; asterisks indicate the zoomed PD shown at the upper right corner of (D) and (H).

proteins were expressed in the presence of a GFP derivative fused to an ER retention signal (HDEL:GFP). Exchanging cytoplasmic GFP with ER-localized HDEL:GFP is expected to impede GFP diffusion if it occurs at the translated protein level (Simpson et al., 2009), but not if it occurs at the level of the HDEL:GFP mRNA. Performing this assay in parallel with both eGFP and HDEL:GFP, it was again observed that eGFP diffused between cells in the presence of either 54K^{CPsV} and 54K^{MiLBVV} whereas HDEL-GFP fluorescence remained restricted to the transformed cell (Fig. 5A and B(iii)). This result indicates that the 54K^{CPsV} and 54K^{MiLBVV} proteins increase the PD SEL allowing cytosolic GFP diffusion, but do not facilitate mRNA movement. Next, we asked whether the 54K^{CPsV} and 54K^{MiLBVV} proteins are able to mediate their own transport through PD. To approach this question, we infiltrated *N. benthamiana* leaves with highly diluted *Agrobacterium* cultures to express either eGFP:54K^{CPsV} (~81 kDa) or eGFP:54K^{MiLBVV} (~82 kDa) in isolated epidermal cells. The molecular sizes of the eGFP fusion proteins exceed the protein size for free cell-to-cell diffusion in source or sink leaves. Surprisingly, the proteins occurred in cell clusters ranging from 2 to 7 cells in 76–77% of the foci analyzed, and the cells in each cluster showed the characteristic PD localization pattern of the fusion proteins (Fig. 5A and B(iv)). The same assay was conducted with CP^{CPsV}:eGFP or CP^{MiLBVV}:eGFP, obtaining fluorescence mainly in single isolated cells with less than 10% foci with 2 or more cells (Fig. 5A and B(v)). Collectively, these results indicate that the 54K^{CPsV} and 54K^{MiLBVV} proteins are NCAPs able to modify the PD SEL thus facilitating their own movement as well as intercellular diffusion of cytoplasmic GFP.

54K^{CPsV} and 54K^{MiLBVV} complement movement-deficient PVX and TMV mutants

The ability to target PD, to move between cells, and to facilitate intercellular trafficking of other macromolecules are hallmark features of viral MPs (Waigmann et al., 1994). To determine if the 54K^{CPsV} and 54K^{MiLBVV} act as ophiovirus MPs, we tested the ability of these proteins to *trans*-complement movement-deficient PVX mutant (pPVX.GUS-Bsp) with a frame-shift mutation in the TGB1/p25 gene (Morozov et al., 1997). Because of the absence of a functional p25, pPVX.GUS-Bsp infection is restricted to the initially infected cells. However, when complemented with p25 the virus can move cell-to-cell leading to GUS expression also in the neighbouring cells (Morozov et al., 1997). When pPVX.GUS-Bsp was loaded together with the empty vector pGD (Goodin et al., 2002) onto microprojectile particles and bombarded into *N. benthamiana* leaves only a low number of GUS foci was observed and most of these foci consisted of single cells. However, when leaves were bombarded with pPVX.GUS-Bsp together with a construct expressing the p25 gene (pRT25 K), the size and number of the GUS foci increased considerably, as previously reported (Fig. 6A) (Morozov et al., 1997). When leaves were bombarded with particles carrying pPVX.GUS-Bsp and either 54K^{CPsV}- or 54K^{MiLBVV}-expressing plasmids (pGD-54K^{CPsV} or pGWB-55 K^{MiLBVV}:FLAG, see Fig. 2), GUS expression occurred in clusters of multiple cells (Fig. 6A). The size and number of GUS-positive clusters obtained were higher than those observed upon co-bombardment with pGD, and similar or smaller than those with p25 (Fig. 6A, Table). Consequently, the results demonstrate that the 54K^{CPsV} and 54K^{MiLBVV} proteins are able to complement the cell-to-cell spread of movement-deficient PVX.

A

	No. of fluorescent foci							% of foci with more than one cell
	1 cell	2 cells	3 cells	4 cells	5 cells	6 cells	7 cells	% movement
GFP	13	2	0	0	0	0	0	13
GFP + CP^{CPsV}	12	0	0	0	0	0	0	0
GFP + CP^{MiLBVV}	14	0	0	0	0	0	0	0
GFP + $54K^{CPsV}$	3	4	7	4	6	3	2	89
GFP + $55K^{MiLBVV}$	4	2	4	8	5	6	3	88
GFP-HDEL	32	4	0	0	0	0	0	11
GFP-HDEL + $54K^{CPsV}$	31	4	1	0	0	0	0	14
GFP-HDEL + $55K^{MiLBVV}$	26	3	0	0	0	0	0	10
eGFP:$54K^{CPsV}$	11	9	4	8	7	3	3	76
eGFP:$55K^{MiLBVV}$	7	5	3	8	3	2	2	77
CP^{CPsV}:eGFP	15	1	0	0	0	0	0	6
CP^{MiLBVV}:eGFP	14	1	0	0	0	0	0	7

B

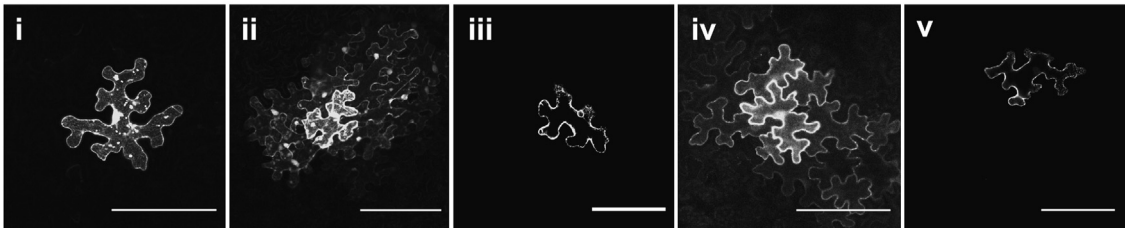

Fig. 5. $54K^{CPsV}$ and $54K^{MiLBVV}$ modify PD SEL and move cell-to-cell. (A) Table indicating the number of GFP-fluorescent foci with the number of cells in each foci for the treatments described in the left column, GFP: pGDG; GFP-HDEL: ER-targeted GFP; CP^{CPsV}: pGD-CP^{CPsV}; CP^{MiLBVV}: CP^{MiLBVV}:FLAG; $54K^{CPsV}$: pGD-$54K^{CPsV}$; $54K^{MiLBVV}$: $54K^{MiLBVV}$:FLAG. (B) Representative images of single cells expressing cytosolic GFP without (i) or with cell-to-cell diffusion (ii), single cells expressing HDEL-GFP (iii), eGFP:$54K^{CPsV}$ showing translocation from the central-expressing to adjacent cells (iv) and single cells expressing CP^{CPsV}:eGFP (v). Scale bar = 150 μm.

No *trans*-complementation was observed upon co-bombardment of the leaves with pPVX.GUS-Bsp together with either CP^{CPsV} or CP^{MiLBVV} (Fig. 6A). These results provide the first functional evidence for a role of $54K^{CPsV}$ and $54K^{MiLBVV}$ in viral cell-to-cell movement.

To further investigate the activity of $54K^{CPsV}$ and $54K^{MiLBVV}$ as ophiovirus MPs we tested the ability of these proteins to *trans*-complement a movement-defective TMV vector that carries a large N-terminal deletion in its MP and which expresses GFP in place of the CP from the CP subgenomic promoter (TMVΔMPΔCP-GFP) (Vogler et al., 2008). Infectious viral RNA transcripts were in vitro-transcribed from cloned viral cDNA and used for rub-inoculation of *N. benthamiana* leaves in the presence of abrasive. The same leaves were agroinfiltrated for *trans*-complementation. Whereas one half of the leaf was agroinfiltrated for the transient expression of $54K^{CPsV}$:mRFP or $54K^{MiLBVV}$:mRFP, the other half of the leaf was agroinfiltrated for the transient expression of MP^{TMV}:mRFP or free mRFP as positive and negative controls, respectively (Fig. 6B). As expected, expression of MP^{TMV}:mRFP but not the expression of free mRFP restored the movement of TMVΔMPΔCP-GFP leading to the expression of GFP fluorescence in clusters of multiple cells (Fig. 6B). A similar functional complementation of TMVΔMPΔCP-GFP movement was also observed upon expression of $54K^{CPsV}$:mRFP or of $54K^{MiLBVV}$:mRFP, whereas no effect was observed upon expression of the ophiovirus CPs (Fig. 6B, Table). These observations confirm the virus cell-to-cell movement function of $54K^{CPsV}$ and $54K^{MiLBVV}$ also seen with our PVX-based assay. Collectively, the above results indicate $54K^{CPsV}$ and $54K^{MiLBVV}$ act as viral MPs.

Homologous interaction between RNA 2-encoded proteins and the ophiovirus CPs

Previously we reported that in the context of CPsV infection or upon the co-expression of FLAG-tagged $54K^{CPsV}$ or $54K^{MiLBVV}$ the cytoplasmic localization of eGFP fused CPs does not change (Peña et al., 2012b). A more extensive analysis was performed by co-expression of both fluorescently tagged CPs with their homologous fluorescently tagged $54K^{CPsV}$ and $54K^{MiLBVV}$, constructs used during this work. Again no relocalization of CPs to PD, nucleus or MT was observed (Fig. S1). Nevertheless, given that the $54K^{CPsV}$ and $54K^{MiLBVV}$ proteins localize to the cytoplasm, we wanted to know whether the cytoplasmic localization could allow an interaction between these MPs and their corresponding CPs. In a first approach we used fluorescence lifetime imaging microscopy (FLIM) to determine if there is a fluorescence resonance energy transfer (FRET) between the eGFP and mRFP moieties of the fusion proteins upon transient expression and localization in the cytoplasm of *N. benthamiana* epidermal cells. The fluorescence lifetime of cytoplasmic eGFP:$54K^{CPsV}$ was 2.54 ns when expressed alone and was reduced to 2.28 ns when the protein was co-expressed with CP^{CPsV}:mRFP, which indicates a FRET efficiency of 10% (Fig. 7A). A similar reduction in the fluorescence lifetime of eGFP signal in the cytoplasm was observed when eGFP:$54K^{MiLBVV}$ was co-expressed with CP^{MiLBVV}:mRFP, indicating a FRET efficiency of 9% (Fig. 7B). Both eGFP:$54K^{CPsV}$ and eGFP:$54K^{MiLBVV}$ showed a very low FRET efficiency with free mRFP (Fig. 7A and B). These observations indicate that both ophiovirus MPs occur in close proximity with their corresponding CP in the cytoplasm of the expressing cells.

Further evidence supporting interactions of $54K^{CPsV}$ or $54K^{MiLBVV}$ with their corresponding virus-specific CPs was obtained by co-immunoprecipitation experiments using RFP-Trap (Chromotek, Germany). As previously reported for CP^{CPsV}:eGFP or CP^{MiLBVV}:eGFP (Peña et al., 2012b), eGFP:$54K^{CPsV}$ and eGFP:$54K^{MiLBVV}$ showed no interaction with free mRFP, as revealed by the absence of the immunoreactive band of 85 kDa in western blot analysis of the bound fraction using anti-GFP antibodies (Fig. 7C and D, left membrane). However, both proteins were co-immunoprecipitated with their homologous CP^{CPsV}:mRFP or

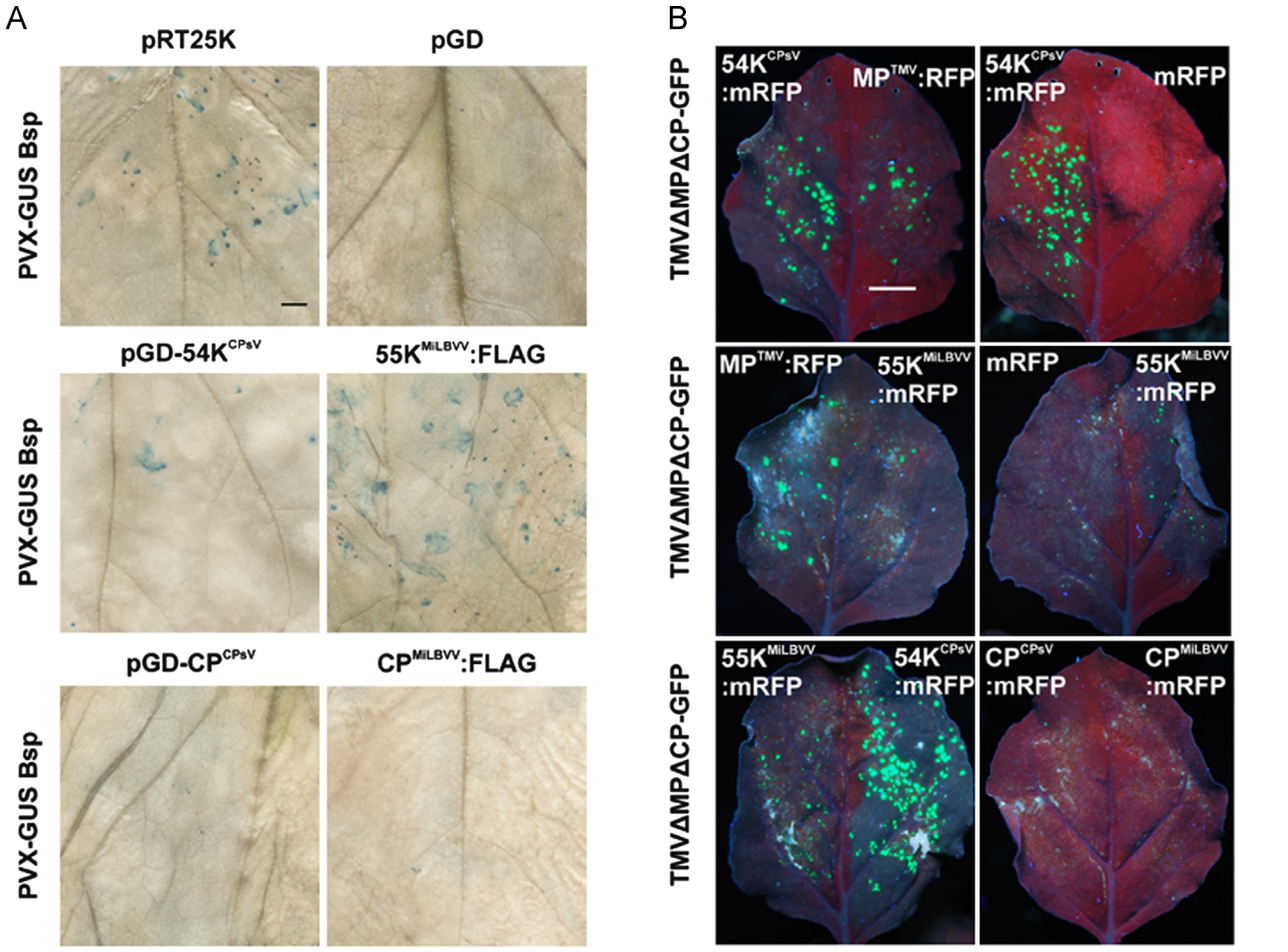

	No. of total foci (No. of foci with a diameter above 200μm)
PVX-GUS Bsp+ pGD	10 (1)
PVX-GUS Bsp + pRT25K	187 (155)
PVX-GUS Bsp + pGD-54K^{CPsV}	46 (20)
PVX-GUS Bsp + 55K^{MiLBVV}-FLAG	153 (112)
PVX-GUS Bsp + pGD-CP^{CPsV}	33 (1)
PVX-GUS Bsp + CP^{MiLBVV}	18 (0)

	No. of total fluorescent foci (No. of foci with a diameter above 200μm)
TMVΔMPΔCP-GFP + mRFP	44 (0)
TMVΔMPΔCP-GFP + MP^{TMV}:RFP	72 (58)
TMVΔMPΔCP-GFP + 54K^{CPsV}:mRFP	308 (280)
TMVΔMPΔCP-GFP + 55K^{MiLBVV}:mRFP	277 (70)
TMVΔMPΔCP-GFP + CP^{CPsV}:mRFP	41 (0)
TMVΔMPΔCP-GFP + CP^{MiLBVV}:mRFP	43 (0)

Fig. 6. 54K^{CPsV} and 54K^{MiLBVV} complement the movement of MP-deficient PVX and TMV. Trans-complementation assay. (A) Representative images of GUS staining of *N. benthamiana* leaves bombarded with the indicated DNA constructs, and table showing the total number of GUS foci and the number of foci with diameters above 200 μm (in brackets) for each viral protein construct co-expressed with PVX.GUS-Bsp. Scale bar = 2 mm. (B) Representative images of UV illuminated *N. benthamiana* leaves inoculated with TMVΔMPΔCP-GFP and agroinfiltrated for the expression of indicated proteins, and table showing the total number of fluorescent foci and the foci with diameters above 200 μm (in brackets) obtained for each protein. Scale bars = 10 mm.

CP^{MiLBVV}:mRFP proteins (Fig. 7C and D, right membrane), indicating interaction. These co-immunoprecipitation results confirm the results obtained by FLIM and indicate that the 54K^{CPsV}and 54K^{MiLBVV} proteins undergo interaction with their corresponding CP.

Discussion

MPs are highly variable in size, amino acid sequence and structure, but they have been described as proteins that accumulate at PD and eventually increase PD SEL mediating virus cell-to-cell and long-distance movement. Here we have demonstrated that the predicted polypeptide encoded by CPsV RNA 2 is present in infected tissue, thus confirming its coding assignment. Attempts to immunolocalize the 54K^{CPsV} and even the CP, well likely more abundant than the 54K^{CPsV}, by polyclonal antisera in thin sections of infected tissue have not been successful (Elliot W. Kitajima, Piracicaba, Brazil, personal communication, and (Peña et al., 2012b)). This outcome/failure could be ascribed to the low virus accumulation (Garcia et al., 1991; Zanek et al., 2006) and the low

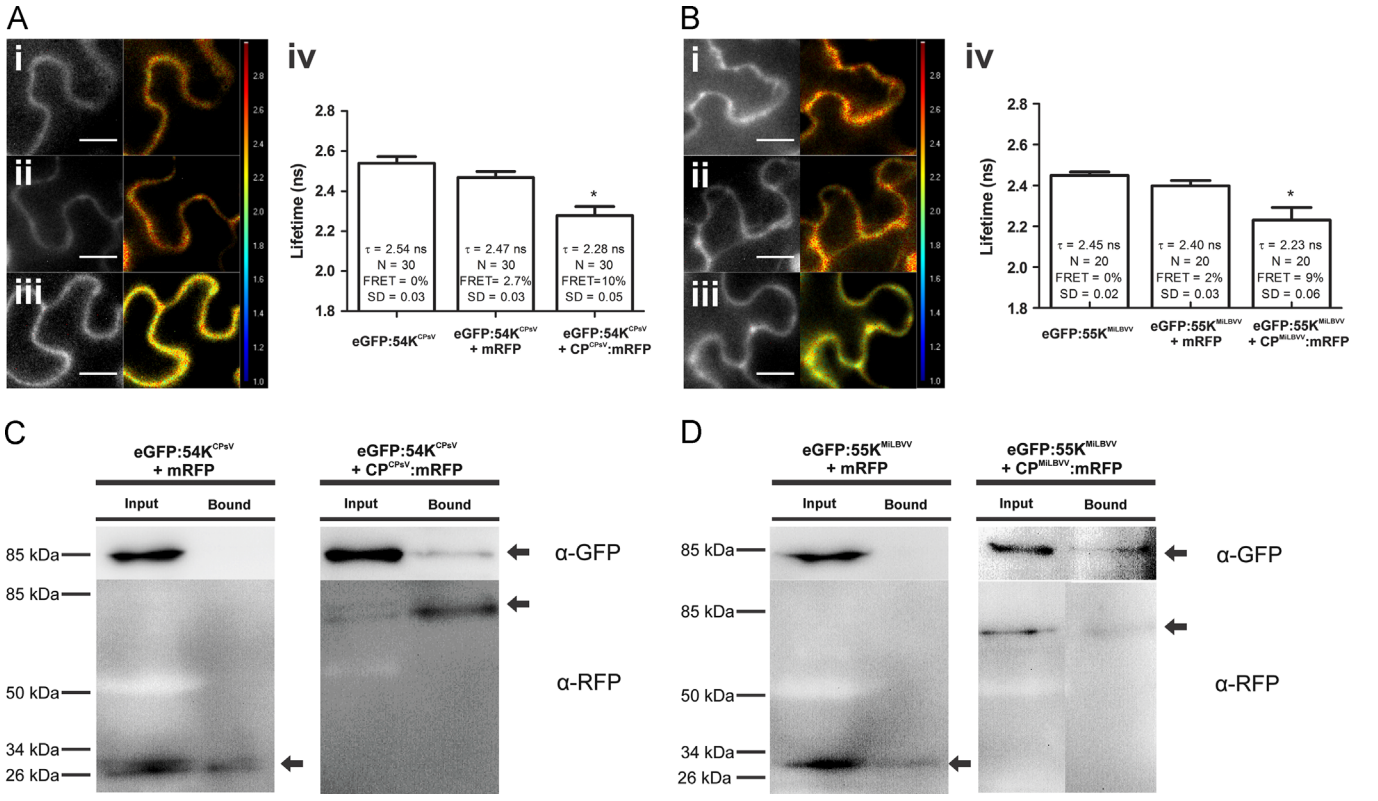

Fig. 7. 54K^{CPsV} and 54K^{MiLBVV} interact with their virus-specific CPs in vivo. FRET-FLIM analysis in *N. benthamiana* epidermal cells. (A) Transiently expressed eGFP:54K^{CPsV} with eGFP fluorescence lifetime values shown in false color if expressed alone (i), or together with mRFP (ii) or with CP^{CPsV}:mRFP (iii) and corresponding numerical values (iv). (B) Transiently expressed eGFP: 54K^{MiLBVV} with eGFP fluorescence lifetime values shown in false color if expressed alone (i) or together with mRFP (ii), or with CP^{MiLBVV}: mRFP (iii), and corresponding numerical values (iv). Fluorescent intensity images (left) are combined with fluorescence lifetime images (right) indicating lifetime in false color code according to the scale (in (A) and (B), right). Scale bar = 10 μm. Lifetime analysis: τ, fluorescent lifetime (ns); SD, standard deviation; *N*, number of cells analyzed. Asterisks represent a significant reduction in eGFP fluorescence lifetime ($p < 0{,}01$). ((C) and (D)) co-immunoprecipitation using mRFP-Trap. Input and Bound fractions were analyzed by immunoblot analysis using anti-GFP (α-GFP) or anti-RFP (α-RFP) antibodies. Interactions tested: (C) eGFP:54K^{CPsV} with CP^{CPsV}:mRFP and (D) eGFP: 54K^{MiLBVV} with CP^{MiLBVV}:mRFP. Molecular weights are indicated to the left. Arrows indicate the corresponding immunoreactive band.

titre of polyclonal antisera assayed (Peña et al., 2012b). Therefore, subcellular localization was addressed by expression of viral proteins tagged with fluorescent proteins and observation by confocal microscopy. This approach was also extended to the 54K protein of MiLBVV. Both proteins were found to localize to PD, a common feature of viral MPs. The observation that cytosolic GFP was able to move to neighbouring cells when co-expressed with 54K^{CPsV} or 54K^{MiLBVV} but restricted to a single cell when either targeted to the ER or expressed alone substantiated the hypothesis that these proteins are MPs. This activity was indeed further confirmed by the ability of the eGFP:54K^{CPsV} and eGFP:54K^{MiLBVV} fusion proteins to mediate their own intercellular movement which again is a feature described for many MPs (Lucas, 2006; Niehl and Heinlein, 2011). Based on these findings we suggest that 54K^{CPsV} or 54K^{MiLBVV} act as ophiovirus MPs.

The function of the 54K^{CPsV} or 54K^{MiLBVV} proteins as MPs was then shown by their ability to provide a movement function to movement-deficient TMV and PVX mutants. Tobamovirus-based vectors were already used previously as a tool for identifying the MPs of negative viruses. For example, the NSvc4 protein of *Rice stripe virus* (RSV) and the protein pC6 of *Rice grassy stunt virus* (RGSV) were shown to *trans*-complement a movement-defective *Tomato mosaic virus* (ToMV) mutant (Hiraguri et al., 2011). Similarly, the NSm protein of *Tomato spotted wilt virus* (TSWV) was shown to complement the cell-to-cell and long distance movement of MP-deficient TMV mutant (Lewandowski and Adkins, 2005). Also PVX.GUS-Bsp (Morozov et al., 1997), which we used here, has been used previously to identify MPs of distant viruses, for example, again the NSvc4 protein of RSV (Xiong et al., 2008), but also the P3 protein of Rice yellow stunt rhabdovirus (RYSV) (Huang et al., 2005) and the S6 protein of *Rice dwarf virus* (RDV) (Li et al., 2004). Because reverse genetic testing has not been established for CPsV and MiLBVV, nor for any other negative-stranded RNA plant virus, the utilization of such *trans*-complementation assays using movement-deficient PVX and TMV viruses represented the best possible way to directly test the MP activity of the 54K^{CPsV} or 54K^{MiLBVV} proteins. Since these proteins act as MPs in the context of both tobamo and potexvirus infection, it appears very likely that these proteins also act as MPs in the context of ophiovirus infection. Movement *trans*-complementation between closely related as well as phylogenetically highly divergent viruses is well documented (Latham and Wilson, 2008). Therefore it is not surprising that the MP of an ophiovirus, that given the negative sense nature of their genomes are supposed to move in a complex containing the viral replicase, can complement TMV or PVX movement deficient virus and supports the movement of replicative complexes (Kawakami et al., 2004). Based on the demonstrated role of RNA 2 encoded protein from CPsV and MiLBVV as MPs, a similar function could be expected for the protein expressed from same genomic location in other members of the *Ophioviridae* family, such as the 50 K protein in LRNV.

In this work we provide evidence regarding the interactions between the two ophiovirus MPs with their corresponding viral CPs. This interaction can be involved in any possible function performed by 54K or 54K, e.g. formation of a transcription-replication complex with RdRp or an active role of CP in the

movement process. CP relocalization, although expected, was not observed upon co-expression with the respective MPs, suggesting that if CP participates in the ophiovirus movement complex other ophiovirus or host factors would also be required to facilitate PD targeting. Such a role would be consistent with several other viruses known to require their CP for movement (Niehl and Heinlein, 2011). The CP can play diverse roles during virus movement. While several virus species require CP as they move between cells in the form of assembled virion, other viruses require the CP for auxiliary function, for example in stabilizing the viral ribonucleprotein complex formed between the viral MP and the viral RNA genome. For instance, the CP of TMV is dispensable for cell-to-cell movement in leaves but plays an essential role in the systemic spread of the virus into distant organs (Niehl and Heinlein, 2011; Peña et al., 2012a). Another example for an auxiliary function of CP is provided by viruses expressing TGB MPs. Whereas the cell-to-cell movement of both hordeiviruses and potexviruses depends on their TGB MPs, only potexviruses like PVX require CP in addition to the TGB MPs for movement. However, whether PVX moves between cells in the form of virion or in the form of a CP-containing ribonucleoprotein complex is yet unclear (Niehl and Heinlein, 2011). Future studies may determine whether and by which role the CP contribute to the cell-to-cell movement of ophioviruses.

The mechanism by which ophioviruses replicate their genomes and target them to PD for intercellular spread also requires further study. We have shown here that the ophiovirus $54K^{CPsV}$ and $54K^{MiLBVV}$ proteins accumulate along microtubules, and subcellular fractionation of CPsV infected tissue indicate that $54K^{CPsV}$ associates with membranes that sediment in the microsomal fraction (unpublished results). The MP^{TMV}, whose movement function was complemented by $54K^{CPsV}$ and $54K^{MiLBVV}$, localizes to viral replication complexes (VRCs) that are formed on the ER early after infection (Heinlein et al., 1998; Mas and Beachy, 1999). These VRCs are anchored to microtubules and at early stages of infection are targeted to PD by actin/myosin-supported lateral diffusion along the ER (Heinlein et al., 1995; Heinlein et al., 1998; Liu et al., 2005; Niehl et al., 2012a; Niehl et al., 2012b; Padgett et al., 1996; Peña and Heinlein, 2012). At later infection stages MP^{TMV} accumulates transiently along microtubules and the ability of the MP^{TMV} to interact with microtubules correlates with MP function in virus movement (Boyko et al., 2000; Niehl et al., 2013; Peña and Heinlein, 2012). In addition to TMV several other viruses were reported to have microtubule-interacting proteins playing a role in virus movement, as examples, the MP of *Tomato mosaic* tobamovirus *Ob* (Padgett et al., 1996), the CP of PVX (Serazev et al., 2003), the TGB1 protein of Potato mop-top pomovirus (Wright et al., 2010), and the Hsp70 protein of Beet yellows closterovirus (Karasev et al., 1992). Unlike TMV, *Grapevine fanleaf virus* or *Cowpea mosaic virus* MPs depend on the secretory pathway to reach PD, as shown by their sensitivity to the secretory pathway inhibitor Brefeldin A (Laporte et al., 2003; Pouwels et al., 2002). It will be exciting to see whether tobamoviruses and ophioviruses share a common pathway for PD targeting.

Our finding that the $54K^{CPsV}$ and $54K^{MiLBVV}$ proteins exhibit intercellular spread and also facilitate the intercellular spread of GFP in *trans* indicates that these proteins have the capacity to alter the SEL of PD. This is a hallmark feature of viral MPs as well as of NCAPs playing a role in plant development (Burch-Smith et al., 2011; Zavaliev et al., 2011). The mechanism by which MPs alter PD SEL is not well understood but likely involves the transient removal of callose deposits from the PD neck region (Epel, 2009; Vaten and Bergmann, 2012; Zavaliev et al., 2011). Recent studies correlated the ability of the MPs of *Cucumber mosaic virus* (CMV) and TMV to sever actin filaments in vitro with increases in PD SEL (Su et al., 2010). However it is unclear whether the implied reorganization of the actin cytoskeleton leading to the SEL increase occurs inside PD and is directly responsible for changing PD permeability. Again, further studies are needed to gain insight into the mechanisms by which the $54K^{CPsV}$ and $54K^{MiLBVV}$ proteins target PD and alter PD SEL for ophiovirus movement.

Materials and methods

Virus isolates and plant inoculation

Young leaves of sweet orange plants (*Citrus sinensis* (L.) Osb) systemically infected with CPsV CPV-4 isolate from Florida (USA) (Garnsey and Timmer, 1980) were used as source of virus for the inoculation of *C. quinoa. Lactuca sativa* leaves infected with MiLBVV-LP2 isolate from La Plata (Argentina) (Barcala Tabarrozzi et al., 2010) were used for total RNA extraction and cloning the ORF present in the RNA2 of MiLBVV-LP2.

Plasmid constructs, bacterial strains and agroinfiltration assays

To express C-terminally tagged fusions of $54K^{CPsV}$ and $54K^{MiLBVV}$, the respective RNA 2 ORFs were amplified without the stop codons by PCR and cloned into pCR8/GW/TOPO (Invitrogen). The same strategy was used to generate the N-terminal fusions but using a reverse primer containing a stop codon. The resulting plasmids were recombined with destination vectors pB7WGF2, pB7RWG2 and pB7FWG2 (Karimi et al., 2002) to obtain N-terminal fusions to eGFP or C-terminal fusions to mRFP or eGFP, or with pGW11 for fusion to a FLAG-tag (Fig. 2), using LR clonase mix (Invitrogen) according to manufacturer's instructions. Correct cloning was confirmed for all constructs by DNA sequencing. Verified constructs were used for transformation of *A. tumefaciens* strain GV3101 by electroporation. Plasmid pBin61-HDEL-GFP was kindly provided by Claude Saint-Jore-Dupas and Veronique Gomord (CNRS, Univ. de Rouen, France).

Transient expression of fusion proteins was obtained upon agroinfiltration of the respective constructs into *N. benthamiana* leaves. *A. tumefaciens* cultures were harvested by centrifugation, resuspended in water to a final $OD_{600\ nm}$ of 0.2 (unless stated differently) and infiltrated into the abaxial side of the leaf, using a syringe without needle. Leaves were observed at 2–3 days post agroinfiltration (dpai).

The expression, size and integrity of the fusion proteins were confirmed by western blot.

Protein analysis

Protein extraction was performed as described previously (Peña et al., 2012b). $54K^{CPsV}$ was detected using polyclonal anti-54 K antiserum (Peña et al., 2012b) as primary antibody and anti-rabbit IgG conjugated to alkaline phosphatase (GibcoBRL, Life Technologies) as secondary antibody followed by incubation with NBT/BCIP (Pierce). eGFP and mRFP fusion proteins were detected with anti-GFP JL-8 monoclonal antibody (BD Biosciences Clontech, USA) and anti-mRFP 3F5 monoclonal antibody, respectively (Chromotek, Germany). Horseradish Peroxidase conjugated anti-mouse (BioRad, USA) was used as secondary antibody. Chemiluminescent reagent was used for developing according to manufacturer's instructions (GE, ECL Plus Western Blotting Detection Reagents, UK).

Fluorescence microscopy

Microscopic techniques, CLSM and FLIM, have been described previously (Peña et al., 2012b). Plasmolysis was accomplished

by infiltration of the plant tissue with a hypertonic solution (30% glycerol) prior to observation.

PD gating assay

PD gating was addressed as described previously (Bayne et al., 2005), with minor modifications. Fully expanded leaves of 5 to 6 week old *N. benthamiana* plants were agroinfiltrated with diluted *A. tumefaciens* cultures carrying either pGDG or pBin61-HDEL:GFP at $OD_{600\ nm}=5\times10^{-4}$ together with pBin61-P19, silencing suppressor (kindly provided by PBL technology, Norwich, UK) (Voinnet et al., 2003) ($OD_{600\ nm}=0,5$) in one half of the leaf, allowing GFP expression in single, isolated epidermal cells, or together with P19 ($OD_{600\ nm}=0,5$) and the protein to be assayed at $OD_{600\ nm}=0,5$, on the other side. To evaluate if CP^{CPsV}, CP^{MiLBVV}, $54K^{CPsV}$ and $54K^{MiLBVV}$ have NCAP activity, leaves were co-infiltrated with a diluted *A. tumefaciens* culture ($OD_{600\ nm}=5\times10^{-4}$) carrying pB7-eGFP:$CP^{CPsV}$, pB7-eGFP:$CP^{MiLBVV}$ (Peña et al., 2012b) pB7-eGFP:$54K^{CPsV}$ or pB7-eGFP:$54K^{MiLBVV}$, both mixed with a culture ($OD_{600\ nm}=0,5$) carrying pBin61-P19. The number of fluorescent foci and cells in each foci were counted three days later by fluorescence microscopy. For these analyses three independent experiments were performed.

PVX and TMV trans-complementation assays

Trans-complementation assays were performed with the movement-deficient PVX construct PVX.GUS-Bsp (kindly provided by Prof. David Baulcombe/SL/The Gatsby Charitable Foundation). Homologous complementation was achieved with p25 as a positive control (Morozov et al., 1997). Particle bombardment was performed using a Biolistic® PDS-100/He (BioRad, USA), according to the manufacturer's instructions. Purified DNA plasmids (PVX.GUS-Bsp and specific protein expression construct) were precipitated on gold particles of 1 μm diameter. Following bombardment of 4 to 5 weeks old *N. benthamiana* leaves, the leaves were kept at 16 h daylight and 23 °C for 2 days, and then stained with X-Gluc according to (Morozov et al., 1997), in three independent experiments, using 4 leaves each protein analyzed. For *trans*-complementation of TMVΔMPΔCP-GFP, the viral cDNA construct was transcribed using the T7 RiboMAX™ transcription kit (Promega) and the infectious RNA rub-inoculated on leaves of 4 to 5 weeks old *N. benthamiana* plants. At 24 h post inoculation the leaves were agroinfiltrated for expression of desired proteins. Infection foci were analyzed 3 dpai and under UV illumination. Two independent experiments were done, each using four treated leaves per protein. A diameter equal or below 200 μm was considered negative for *trans*-complementation of the movement-deficient PVX or TMV constructs. Foci with diameter above this value were considered positive for *trans*-complementation.

Co-immunoprecipitation assays

Co-immunoprecipitation assays were performed with RFP-Trap A as described by the manufacturer (Chromotek, Germany), with minor modifications (Peña et al., 2012b). Bound and Input fractions were analyzed as described under Protein analysis.

Acknowledgments

We thank the Functional Genomics Division of the Department of Plant Systems Biology at the VIB-Ghent University for providing plasmids pB7FWG2, pB7RWG2 and pB7WGF2, M. M. Goodin for providing the pGD vector, and EW Kitajima for the attempts to immunolocalize $54K^{CPsV}$ using TEM. We would like to thank Dr. Fernando Bravo Almonacid, Dr. Mariana del Vas and Dr. Vanesa Mongelli for their help with the particle bombardment assays, and Celina Castuma for her help in the manuscript revision. M. L. García and Gabriel Robles Luna belong to the staff of Departamento de Ciencias Biológicas, Facultad de Ciencias Exactas (UNLP), and Maria Laura Garcia is researcher of CONICET. G. Robles Luna is a fellow of CONICET. This work was performed with financial support of ANPCyT and CONICET (grants PICT 11714, PICT 32359, PICT 1094 and PIP 6108) in Argentina, and by the CNRS and the ANR (grant ANR-08-BLAN-0244) in France. The authors thank the EMBO for financial support through a short-term fellowship to Gabriel Robles Luna to work in the laboratory of M. Heinlein at the IBMP (CNRS UPR2357) in Strasbourg, France.

Appendix A. Supporting information

Supplementary data associated with this article can be found in the online version at http://dx.doi.org/10.1016/j.virol.2013.03.019.

References

Alioto, D., Guerri, J., Moreno, P., Milne, R.G., 2007. Citrus psorosis virus. In: Rao, G.P., Myrta, A., Ling, K.S. (Eds.), Characterization, Diagnosis and Management of Plant Viruses. Studium Press LL. C., Houston, TX, USA.

Barcala Tabarrozzi, A.E., Peña, E.J., Dal, Bo, E., Robles Luna, G., Reyes, C.A., Garcia, M. L., 2010. Identification of *Mirafiori lettuce big-vein virus* and *Lettuce big-vein associated virus* infecting *Lactuca sativa* with symptoms of lettuce big-vein disease in Argentina. Plant Pathol. 59, 1160–1161.

Bayne, E.H., Rakitina, D.V., Morozov, S.Y., Baulcombe, D.C., 2005. Cell-to-cell movement of *Potato Potexvirus X* is dependent on suppression of RNA silencing. Plant Journal: Cell Mol. Biol. 44, 471–482.

Bos, L., Huijberts, N., 1996. Lettuce ring necrosis, caused by a chytrid-borne agent distinct from *Lettuce big-vein virus*. Eur. J. Plant Pathol. 102, 867–873.

Boyko, V., Ferralli, J., Ashby, J., Schellenbaum, P., Heinlein, M., 2000. Function of microtubules in intercellular transport of plant virus RNA. Nat. Cell Biol. 2, 826–832.

Burch-Smith, T.M., Stonebloom, S., Xu, M., Zambryski, P.C., 2011. Plasmodesmata during development: re-examination of the importance of primary, secondary, and branched plasmodesmata structure versus function. Protoplasma 248, 61–74.

Deom, C.M., Oliver, M.J., Beachy, R.N., 1987. The 30-kilodalton gene product of *Tobacco mosaic virus* potentiates virus movement. Science 237, 389–394.

Derrick, P.M., Barker, H., Oparka, K.J., 1992. Increase in plasmodesmatal permeability during cell-to-cell spread of *Tobacco rattle virus* from individually inoculated cells. Plant Cell 4, 1405–1412.

Epel, B.L., 2009. Plant viruses spread by diffusion on ER-associated movement-protein-rafts through plasmodesmata gated by viral induced host beta-1,3-glucanases. Semin. Cell Dev. Biol. 20, 1074–1081.

Garcia, M.L., Grau, O., Sarachu, A.N., 1991. *Citrus psorosis* is probably caused by a bipartite ssRNA virus. Res. Virol. 142, 303–311.

Garnsey, S.M., Timmer, L.W., 1980. Mechanical transmissibility of Citrus ringspot virus isolates from Florida, Texas, and California. In: Calavan, E.C., Garnsey, S.M., Timmer, L.W. (Eds.), Proceedings of the Eighth Conference of the International Organization of Citrus Virologists. IOCV, Riverside, CA, pp. 174–179.

Goodin, M.M., Dietzgen, R.G., Schichnes, D., Ruzin, S., Jackson, A.O., 2002. pGD vectors: versatile tools for the expression of green and red fluorescent protein fusions in agroinfiltrated plant leaves. Plant J: Cell Mol. Biol. 31, 375–383.

Heinlein, M., Epel, B.L., Padgett, H.S., Beachy, R.N., 1995. Interaction of tobamovirus movement proteins with the plant cytoskeleton. Science 270, 1983–1985.

Heinlein, M., Padgett, H.S., Gens, J.S., Pickard, B.G., Casper, S.J., Epel, B.L., Beachy, R. N., 1998. Changing patterns of localization of the *Tobacco mosaic virus* movement protein and replicase to the endoplasmic reticulum and microtubules during infection. Plant Cell 10, 1107–1120.

Hiraguri, A., Netsu, O., Shimizu, T., Uehara-Ichiki, T., Omura, T., Sasaki, N., Nyunoya, H., Sasaya, T., 2011. The nonstructural protein pC6 of Rice grassy stunt virus *trans*-complements the cell-to-cell spread of a movement-defective tomato mosaic virus. Arch. Virol. 156, 911–916.

Huang, Y.W., Geng, Y.F., Ying, X.B., Chen, X.Y., Fang, R.X., 2005. Identification of a movement protein of rice yellow stunt rhabdovirus. J. Virol. 79, 2108–2114.

Karasev, A.V., Kashina, A.S., Gelfand, V.I., Dolja, V.V., 1992. HSP70-related 65 kDa protein of beet yellows closterovirus is a microtubule-binding protein. FEBS Lett. 304, 12–14.

Karimi, M., Inze, D., Depicker, A., 2002. GATEWAY vectors for *Agrobacterium*—mediated plant transformation. Trends Plant Sci. 7, 193–195.

Kawakami, S., Watanabe, Y., Beachy, R.N., 2004. *Tobacco mosaic virus* infection spreads cell to cell as intact replication complexes. Proc. Nat. Acad. Sci. U.S.A. 101, 6291–6296.

Kormelink, R., Garcia, M.L., Goodin, M., Sasaya, T., Haenni, A.L., 2011. Negative-strand RNA viruses: the plant-infecting counterparts. Virus Res. 162, 184–202.
Laporte, C., Vetter, G., Loudes, A.M., Robinson, D.G., Hillmer, S., Stussi-Garaud, C., Ritzenthaler, C., 2003. Involvement of the secretory pathway and the cytoskeleton in intracellular targeting and tubule assembly of *Grapevine fanleaf virus* movement protein in tobacco BY-2 cells. Plant Cell 15, 2058–2075.
Latham, J.R., Wilson, A.K., 2008. Transcomplementation and synergism in plants: implications for viral transgenes? Mol. Plant Pathol. 9, 85–103.
Lewandowski, D.J., Adkins, S., 2005. The tubule-forming NSm protein from *Tomato spotted wilt virus* complements cell-to-cell and long-distance movement of *Tobacco mosaic virus* hybrids. Virology 342, 26–37.
Li, Y., Bao, Y.M., Wei, C.H., Kang, Z.S., Zhong, Y.W., Mao, P., Wu, G., Chen, Z.L., Schiemann, J., Nelson, R.S., 2004. Rice dwarf phytoreovirus segment S6-encoded nonstructural protein has a cell-to-cell movement function. J. Virol. 78, 5382–5389.
Liu, J.Z., Blancaflor, E.B., Nelson, R.S., 2005. The *Tobacco mosaic virus* 126-kilodalton protein, a constituent of the virus replication complex, alone or within the complex aligns with and traffics along microfilaments. Plant Physiol. 138, 1853–1865.
Lot, H., Campbell, R.N., Souche, S., Milne, R.G., Roggero, P., 2002. Transmission by *Olpidium brassicae* of *Mirafiori lettuce* virus and Lettuce big-vein virus, and their roles in *Lettuce big-vein etiology*. Phytopathology 92, 288–293.
Lucas, W.J., 2006. Plant viral movement proteins: agents for cell-to-cell trafficking of viral genomes. Virology 344, 169–184.
Lucas, W.J., Ham, B.K., Kim, J.Y., 2009. Plasmodesmata - bridging the gap between neighboring plant cells. Trends Cell Biol. 19, 495–503.
Mas, P., Beachy, R.N., 1999. Replication of *Tobacco mosaic virus* on endoplasmic reticulum and role of the cytoskeleton and virus movement protein in intracellular distribution of viral RNA. J. Cell Biol. 147, 945–958.
Maule, A.J., Benitez-Alfonso, Y., Faulkner, C., 2011. Plasmodesmata—membrane tunnels with attitude. Curr. Opin. Plant Biol. 14, 683–690.
Meshi, T., Watanabe, Y., Saito, T., Sugimoto, A., Maeda, T., Okada, Y., 1987. Function of the 30 kd protein of *Tobacco mosaic virus*: involvement in cell-to-cell movement and dispensability for replication. EMBO J. 6, 2557–2563.
Morozov, S., Fedorkin, O.N., Juttner, G., Schiemann, J., Baulcombe, D.C., Atabekov, J. G., 1997. Complementation of a *Potato virus X* mutant mediated by bombardment of plant tissues with cloned viral movement protein genes. J. Gen. Virol. 78 (Pt 8), 2077–2083.
Naum-Ongania, G., Gago-Zachert, S., Peña, E., Grau, O., Garcia, M.L., 2003. *Citrus psorosis virus* RNA 1 is of negative polarity and potentially encodes in its complementary strand a 24 K protein of unknown function and 280 K putative RNA dependent RNA polymerase. Virus Res. 96, 49–61.
Niehl, A., Amari, K., Gereige, D., Brandner, K., Mely, Y., Heinlein, M., 2012a. Control of *Tobacco mosaic virus* movement protein fate by cell-division-cycle protein 48 (CDC48). Plant Physiol.
Niehl, A., Amari, K., Heinlein, M., 2012b. CDC48 function during TMV infection: Regulation of virus movement and replication by degradation? Plant Signal Behav., 8.
Niehl, A., Heinlein, M., 2011. Cellular pathways for viral transport through plasmodesmata. Protoplasma 248, 75–99.
Niehl, A., Peña, E.J., Amari, K., Heinlein, M., 2013. Microtubules in viral replication and transport. Plant J.: Cell Mol. Biol..
Oparka, K.J., Roberts, A.G., Boevink, P., Santa Cruz, S., Roberts, I., Pradel, K.S., Imlau, A., Kotlizky, G., Sauer, N., Epel, B., 1999. Simple, but not branched, plasmodesmata allow the nonspecific trafficking of proteins in developing tobacco leaves. Cell 97, 743–754.
Padgett, H.S., Epel, B.L., Kahn, T.W., Heinlein, M., Watanabe, Y., Beachy, R.N., 1996. Distribution of tobamovirus movement protein in infected cells and implications for cell-to-cell spread of infection. Plant J.: Cell Mol. Biol. 10, 1079–1088.
Peña, E., Niehl, A., Heinlein, M., 2012a. Viral studies point the way: mechanisms of intercellular transport. In: Kragler, F., Hülskamp, M. (Eds.), Short and Long Distance Signaling. Springer, New York, pp. 1–43.
Peña, E.J., Heinlein, M., 2012. RNA transport during TMV cell-to-cell movement. Front. Plant Sci. 3, 193.
Peña, E.J., Robles Luna, G., Zanek, M.C., Borniego, M.B., Reyes, C.A., Heinlein, M., Garcia, M.L., 2012b. *Citrus psorosis* and *Mirafiori lettuce big-vein* ophiovirus coat proteins localize to the cytoplasm and self interact in vivo. Virus Res..
Poirson, A., Turner, A.P., Giovane, C., Berna, A., Roberts, K., Godefroy-Colburn, T., 1993. Effect of the *Alfalfa mosaic virus* movement protein expressed in transgenic plants on the permeability of plasmodesmata. J. Gen. Virol. 74 (Pt 11), 2459–2461.
Pouwels, J., Van Der Krogt, G.N., Van Lent, J., Bisseling, T., Wellink, J., 2002. The cytoskeleton and the secretory pathway are not involved in targeting the *Cowpea mosaic virus* movement protein to the cell periphery. Virology 297, 48–56.
Roggero, P., Ciuffo, M., Vaira, A.M., Accotto, G.P., Masenga, V., Milne, R.G., 2000. An Ophiovirus isolated from lettuce with big-vein symptoms. Arch. Virol. 145, 2629–2642.
Sánchez de la Torre, E., Riva, O., Zandomeni, R., Grau, O., García, M.L., 1998. The top component of *Citrus psorosis virus* contains two ssRNAs, the smaller encodes the coat protein, Mol. Plant Pathol. On-Line.
Sánchez de la Torre, M.E., Lopez, C., Grau, O., Garcia, M.L., 2002. RNA 2 of *Citrus psorosis virus* is of negative polarity and has a single open reading frame in its complementary strand. J. Gen. Virol. 83 (Pt 7), 1777–1781.
Serazev, T.V., Nadezhdina, E.S., Shanina, N.A., Leshchiner, A.D., Kalinina, N.O., Morozov, S., 2003. [Virions and membrane proteins of the *Potato virus X* interact with microtubules and enables tubulin polymerization in vitro]. Mol. Biol. (Mosk) 37, 1080–1088.
Simpson, C., Thomas, C., Findlay, K., Bayer, E., Maule, A.J., 2009. An Arabidopsis GPI-anchor plasmodesmal neck protein with callose binding activity and potential to regulate cell-to-cell trafficking. Plant Cell 21, 581–594.
Su, S., Liu, Z., Chen, C., Zhang, Y., Wang, X., Zhu, L., Miao, L., Wang, X.C., Yuan, M., 2010. *Cucumber mosaic virus* movement protein severs actin filaments to increase the plasmodesmal size exclusion limit in tobacco. Plant Cell 22, 1373–1387.
Thomas, C.L., Bayer, E.M., Ritzenthaler, C., Fernandez-Calvino, L., Maule, A.J., 2008. Specific targeting of a plasmodesmal protein affecting cell-to-cell communication. PLoS Biol. 6, e7.
Torok, V.A., Vetten, H.I., 2010. Ophiovirus Associated with *Lettuce ring necrosis*, European Society for Virology Meeting, Cernobbio, Italy, p. 282.
Torok, V.A., Vetten, H.J., 2002. Characterisation of an ophiovirus associated with *Lettuce ring necrosis*. In: Joint Conference International Working Groups on Legume and Vegetable Viruses, Bonn, Germany, p. 4.
Torok, V.A., Vetten, J., 2003. Identification and molecular characterisation of a new ophiovirus associated with *Lettuce ring necrosis* disease. In: Proceedings of Arbeitskreis Viruskrankheiten der Pflanzen, Heidelberg, Germany.
Vaira, A.M., Hansen, M.A., Murphy, C., Reinsel, M.D., Hammond, J., 2009. First Report of *Freesia sneak virus* in Freesia sp. in Virginia, USA. Plant Disease Report 93, 965.
Vaira, A.M., Kleynhans, R., Hammond, J., 2007. First Report of *Freesia sneak virus* infecting Lachenalia cultivars in South Africa. Plant Disease Report 91, 770.
Van Damme, D., Van Poucke, K., Boutant, E., Ritzenthaler, C., Inze, D., Geelen, D., 2004. In vivo dynamics and differential microtubule-binding activities of MAP65 proteins. Plant Physiol. 136, 3956–3967.
van der Wilk, F., Dullemans, A.M., Verbeek, M., van den Heuvel, J.F., 2002. Nucleotide sequence and genomic organization of an ophiovirus associated with lettuce big-vein disease. J. Gen. Virol. 83, 2869–2877.
van Dorst, H.J.M., 1975. Evidence for the soil-borne nature of *Freesia leaf necrosis virus*. Neth. J. Plant Pathol. 81, 45–48.
Vaquero, C., Turner, A.P., Demangeat, G., Sanz, A., Serra, M.T., Roberts, K., Garcia-Luque, I, 1994. The 3a protein from *Cucumber mosaic virus* increases the gating capacity of plasmodesmata in transgenic tobacco plants. J. Gen. Virol. 75 (Pt 11), 3193–3197.
Vaten, A., Bergmann, D.C., 2012. Mechanisms of stomatal development: an evolutionary view. Evodevo 3, 11.
Vogler, H., Kwon, M.O., Dang, V., Sambade, A., Fasler, M., Ashby, J., Heinlein, M., 2008. *Tobacco mosaic virus* movement protein enhances the spread of RNA silencing. PLoS Pathog. 4, e1000038.
Voinnet, O., Rivas, S., Mestre, P., Baulcombe, D., 2003. An enhanced transient expression system in plants based on suppression of gene silencing by the p19 protein of *Tomato bushy stunt virus*. Plant Journal: Cell Mol. Biol. 33, 949–956.
Waigmann, E., Lucas, W.J., Citovsky, V., Zambryski, P., 1994. Direct functional assay for *Tobacco mosaic virus* cell-to-cell movement protein and identification of a domain involved in increasing plasmodesmal permeability. Proc. Nat. Acad. Sci. U.S.A. 91, 1433–1437.
Wolf, S., Deom, C.M., Beachy, R.N., Lucas, W.J., 1989. Movement protein of *Tobacco mosaic virus* modifies plasmodesmatal size exclusion limit. Science 246, 377–379.
Wright, K.M., Cowan, G.H., Lukhovitskaya, N.I., Tilsner, J., Roberts, A.G., Savenkov, E. I., Torrance, L., 2010. The N-terminal domain of PMTV TGB1 movement protein is required for nucleolar localization, microtubule association, and long-distance movement. Mol. Plant-Microbe Interact. 23, 1486–1497.
Xiong, R., Wu, J., Zhou, Y., Zhou, X., 2008. Identification of a movement protein of the *Tenuivirus* Rice stripe virus. J. Virol. 82, 12304–12311.
Zanek, M.C., Peña, E., Reyes, C.A., Figueroa, J., Stein, B., Grau, O., Garcia, M.L., 2006. Detection of *Citrus psorosis virus* in the northwestern citrus production area of Argentina by using an improved TAS-ELISA. J. Virol. Methods 137, 245–251.
Zavaliev, R., Ueki, S., Epel, B.L., Citovsky, V., 2011. Biology of callose (beta-1,3-glucan) turnover at plasmodesmata. Protoplasma 248, 117–130.